

## Ab initio phonon dispersion relations of $\alpha$ -Ga

I. Spagnolatti and M. Bernasconi<sup>a</sup>

Dipartimento di Scienza dei Materiali and Istituto Nazionale per la Fisica della Materia, Università degli Studi di Milano-Bicocca, Via Cozzi 53, 20125 Milano, Italy

Received 29 July 2003

Published online 19 November 2003 – © EDP Sciences, Società Italiana di Fisica, Springer-Verlag 2003

**Abstract.** We present the ab initio phonon dispersion relations of  $\alpha$ -Ga. The calculations are carried out within density functional perturbation theory by using either norm-conserving pseudopotential and 4s and 4p electrons in the valence or ultrasoft pseudopotential and 3d electrons in the valence as well. The inclusion of 3d electrons in the valence turned out to be necessary to better reproduce the experimental frequencies of the stretching modes of the Ga<sub>2</sub> dimers present in the  $\alpha$ -Ga structure.

**PACS.** 63.20.Dj Phonon states and bands, normal modes, and phonon dispersion – 71.15.Nc Total energy and cohesive energy calculations – 71.15.Mb Density functional theory, local density approximation, gradient and other corrections

Gallium is a trivalent metal with an unusual crystal structure in the stable low pressure phase, called  $\alpha$ -Ga. The *Cmca* structure of the  $\alpha$  phase is commonly described in terms of the face-centered orthorhombic unit cell with eight atoms per cell reported in Figure 1 [1,2]. A peculiar feature is that each atom has only one nearest neighbor at a distance of 2.44 Å. The second, third and fourth shells each contains two atoms, and are 0.27 Å, 0.30 Å, and 0.39 Å further apart. These six atoms can be seen as lying on a strongly buckled plane, about 1.9 Å thick, perpendicular to the [010] direction. Each atom in these strongly buckled planes is pairwise connected through a short bond to its first neighbor on the adjacent plane. The distance between nearest-neighbor atom pairs is comparatively short for a normal metallic bond, which foreshadow the covalent nature of this bond [4,5]. In the extreme covalent picture the Ga<sub>2</sub> pairs can be seen as dimers, making  $\alpha$ -Ga the only elemental solid exhibiting both metallic and “molecular” behavior at low pressure. This view is supported by several physical properties, for instance, the much higher electrical and thermal conductivity in the “metallic” (010) planes [6], the sharp peak in optical reflectivity typical of a bonding-antibonding transition [7], and the low density of states at the Fermi level from angle-integrated photoemission [8]. Theoretically, a partial covalent character was first suggested by interpretation of the band structure calculations based on empirical pseudopotentials [4,7,9] and then confirmed by modern density-functional-based calculations [10]. Electronic band structure from the latter ab initio calculations [10] is in good agreement with recent angle-resolved photoemission measurements [11].

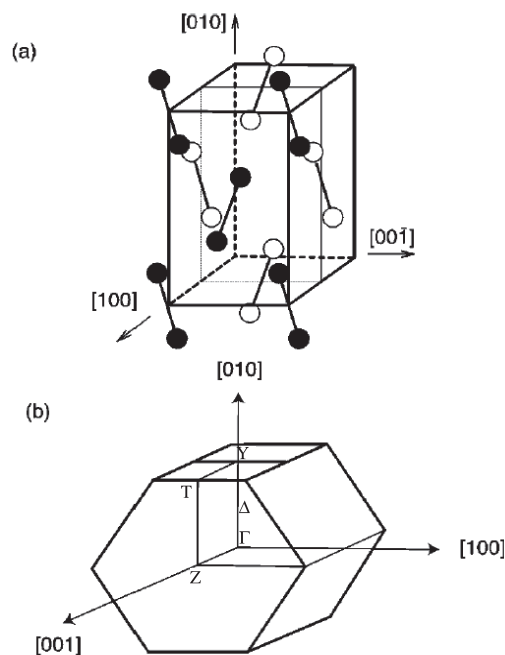


**Fig. 1.** (a) Face-centered orthorhombic cell of  $\alpha$ -Ga. Each site is occupied by a Ga<sub>2</sub>-dimer. Filled circles represent atoms lying on the (100) plane at  $x = a$ , while open circle atoms lie on the next lower plane at  $x = a/2$ . Atoms in the  $x = 0$  plane are in the same positions of those at  $x = a$  and are not shown. (b) Brillouin Zone of  $\alpha$ -Ga [3].

A further support to the description of  $\alpha$ -Ga in terms of a metallic molecular crystal comes from the analysis of its vibrational properties. Phonon dispersion relations measured by inelastic neutron scattering [12] (Fig. 2) show

<sup>a</sup> e-mail: marco.bernasconi@unimib.it

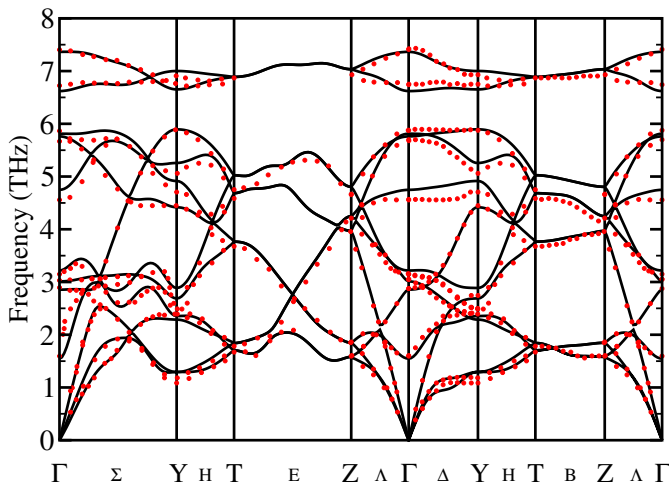


**Fig. 2.** (Color in the online version) Theoretical (black lines) and experimental (red dots from Ref. [12]) phonon dispersion relations of  $\alpha$ -Ga along high symmetry directions in the Brillouin Zone (cf. Fig. 1b). Theoretical frequencies have been computed with the Ultrasoft pseudopotential (USP) including  $3d$  electrons in the valence. A  $8 \times 8 \times 8$  and  $5 \times 5 \times 5$  meshes in  $\mathbf{k}$ - and  $\mathbf{q}$ -space have been used, respectively (see text). For points and directions of the Brillouin Zone, we have used the standard notation for the  $Cmca$  space group (N. 64) as reported for instance in reference [23], as opposed to experimental work of reference [12] where the notation for the non-standard  $Bbcm$  setting has been used.

two high frequency bands separated by a  $\sim 2$  THz gap from the other bands at lower frequencies. The two high frequency bands have been assigned to stretching frequencies of the two  $\text{Ga}_2$  dimers per unit cell.

In this paper we continue our ab initio investigation on the properties of metallic Ga, started with the study in reference [10], by reporting the ab initio calculation of the phonon dispersion relations in  $\alpha$ -Ga. Calculations have been performed within density functional perturbation theory (DFPT) [13–15]. The local density approximation (LDA) has been adopted. We have performed calculations with both a norm conserving pseudopotential (NCP) with  $4s$  and  $4p$  electrons in the valence [10] and with an ultrasoft pseudopotential (USP) [17] including also  $3d$  electrons in the valence. Kohn-Sham orbitals are expanded in plane waves up to a kinetic cutoff of 14 Ry and 30 Ry for NCP and USP, respectively. The inclusion of the  $3d$  electrons in the valence turned out to be necessary to reproduce the experimental frequencies of the highest energy modes which are largely underestimated with NCP, as described below.

The equilibrium geometry and bulk modulus calculated with NCP and USP are compared with experimental data in Table 1. The equilibrium volume has been obtained from a fit of the total energy as a function of volume with the Murnaghan function [20]. At each volume the  $b/a$  and  $c/a$  ratios have been optimized by a linear extrapolation of the anisotropic part of the stress tensor ( $\sigma_{xx} - \sigma_{yy}$  and  $\sigma_{xx} - \sigma_{zz}$ ). Residual anisotropy in the stress at the chosen equilibrium configuration is below 1 kbar. Integration over the Brillouin Zone (BZ) for geom-

**Table 1.** Experimental (from Refs. [1,16]) and theoretical structural parameters of  $\alpha$ -Ga for norm-conserving pseudopotential (NCP) with  $4s$  and  $4p$  electrons in the valence and ultrasoft pseudopotential (USP) including  $3d$  electrons in the valence.  $a, b, c$  are lattice parameters,  $u$  and  $v$  are internal structural parameters [1],  $d$  is the length of the  $\text{Ga}_2$  dimer and  $\theta$  its tilting angle with respect to the  $[010]$  direction,  $V_0$  is the equilibrium volume. Lengths are in  $\text{\AA}$  and angles in degrees.

	NCP	USP	Exp.
$a$	4.326	4.424	4.510
$b$	7.392	7.498	7.645
$c$	4.373	4.431	4.516
$u$	0.1557	0.1558	0.1525
$v$	0.0797	0.0839	0.0785
$d$	2.405	2.451	2.437
$\theta$	16.19	17.65	16.91
$V_0$	17.49	18.37	19.46

etry optimization has been performed over a  $12 \times 12 \times 12$  Monkhorst-Pack (MP) mesh [18]. The smearing technique of reference [19] with smearing parameter  $\sigma = 0.02$  Ry and first-order approximant to the  $\delta$ -function has been used. Zero-point motion are not included in geometry optimization. As discussed in our previous work [10], the equilibrium volume obtained with NCP (only  $4s$  and  $4p$  electrons in the valence) is  $\sim 10\%$  lower than the experimental value. Non-linear-core correction with still frozen  $3d$  electrons in the core does not cure the misfit [10]. Inclusion of gradient corrections does not improve the situation either [10]. In fact, by adding Becke-Perdew gradient corrections [21], the theoretical equilibrium volume ( $19.56 \text{ \AA}^3$ ) becomes slightly larger than the experimental value, but the bulk modulus and the stretching frequencies of the  $\text{Ga}_2$  dimers are largely underestimated which make the overall agreement with experiments worse than within LDA [10]. Conversely, the inclusion of  $3d$  electrons in the valence substantially improves the agreement with experimental structural data (cf. Tab. 1) and also allow to satisfactorily reproduce the phononic bands as reported in Figure 2. In the calculation of phonon dispersion relations of Figure 2 the integration over the BZ has been performed on a coarser  $8 \times 8 \times 8$  MP mesh in  $\mathbf{k}$ -space. The dynamical matrices have been computed on a  $5 \times 5 \times 5$  grid in  $\mathbf{q}$ -space. A Fourier interpolation technique provided the dynamical matrix at the other points of the BZ [13]. The phonon calculations with USP including  $3d$  electrons in the valence are computationally very demanding and the grids in  $\mathbf{k}$ - and  $\mathbf{q}$ -space quoted above are the largest we could afford (the data reported in Figure 2 required 3000 hours-node on an IBM SP3). However, the latter grids, especially that in  $\mathbf{q}$ -space used for the Fourier interpolation, are still not large enough to reach the accuracy achievable within DFPT. In fact, the misfit with experimental data in Figure 2 can be partially accounted for by an insufficient convergence with respect grid sizes. The errors introduced by the size of  $\mathbf{k}$ - and  $\mathbf{q}$ -space grids have been quantified by computing phononic bands with the less computationally demanding NCP. Figure 3 reports the phononic bands computed with NCP with two grid sizes: the same grids

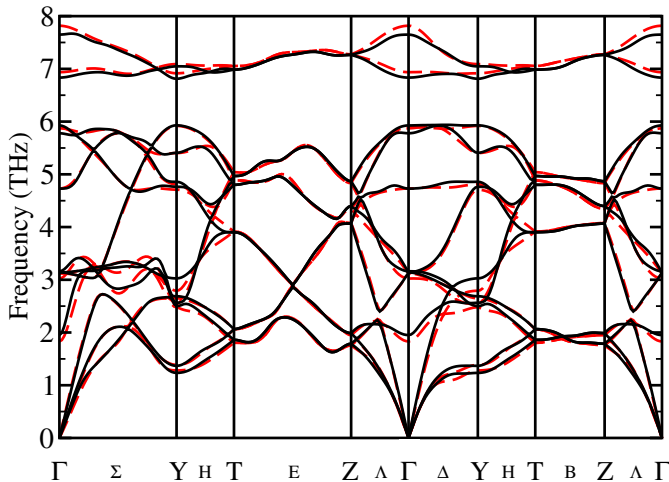


**Fig. 3.** (Color) Phonon dispersion relations of  $\alpha$ -Ga computed with norm conserving pseudopotential (NCP) and  $3d$  electrons frozen in the core with the same mesh used for the calculation reported in Figure 2 (red dashed lines) and at full convergence (black lines) in the  $\mathbf{k}$ - and  $\mathbf{q}$ -space meshes ( $12 \times 12 \times 12$  and  $8 \times 8 \times 8$ , respectively).

used for the USP calculation in Figure 2 (red dashed lines) and the finer  $12 \times 12 \times 12$  and  $8 \times 8 \times 8$  MP grids in  $\mathbf{k}$ - and  $\mathbf{q}$ -space, respectively (black lines), which guarantee full convergence of phonon frequencies (within 0.05 THz). Deviations from fully converged frequencies in Figure 3 are largest for the acoustic bands near point  $Y$  along  $\Delta$ , for bands at  $\sim 4$  THz close to point  $T$  along  $H$ , and for the dimer stretching modes at  $\Gamma$ . Inspection of the calculated phonon displacement patterns at the  $\Gamma$  point confirmed indeed that the higher (lower) phononic band in the range 6.7–7.4 THz correspond to an in-phase (out-of-phase) stretching mode of the two dimers in the unit cell. For sake of completeness we compare in Figure 4 the phononic bands computed with USP and NCP with the same meshes used in the calculation reported in Figure 2 ( $8 \times 8 \times 8$  and  $5 \times 5 \times 5$  for  $\mathbf{k}$ - and  $\mathbf{q}$ -space, respectively). The largest change in the phononic bands due to the inclusion of  $3d$  electrons in the valence is the softening of the dimer stretching bands (cf. Fig. 4). Inclusion of  $3d$  electrons also produces a sizable softening of phonons in the range 1.5–5 THz at point  $T$  which are brought to a better agreement with experiments. Comparison of Figures 2–4 suggest that an insufficient  $\mathbf{k}$  and (mainly)  $\mathbf{q}$  sampling is responsible for the misfit of USP results with respect to experiments for the acoustic bands close to  $Y$  along  $\Delta$ , for bands at  $\sim 2.5$  THz close to  $Y$  and bands at  $\sim 4$  THz close to  $T$ .

In summary, ab initio phonon dispersion relations of  $\alpha$ -Ga are in satisfactory agreement with experimental data provided that  $3d$  electrons are explicitly included in the valence. Residual misfit with respect to experimental data for particular phonons, also considering the errors introduced by  $\mathbf{q}$  and  $\mathbf{k}$  meshes as described above, are still larger than usual for DFPT calculations on simple metals [13], although experimental uncertainties comparable to the misfit are also possible (error bars are not given in the

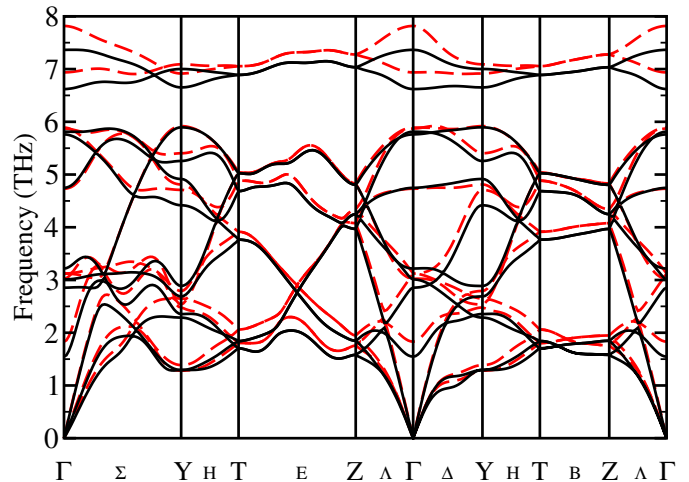


**Fig. 4.** (Color) Phonon dispersion relations of  $\alpha$ -Ga computed with the same  $\mathbf{k}$ - and  $\mathbf{q}$ -space meshes for NCP (red dashed lines, the same as in Fig. 3) and for USP (black lines, the same as in Fig. 2).

experimental data of Ref. [12]). These results are a further indication [10] that the competition between metallic and covalent bonding make gallium a particularly severe system to test the accuracy of DFT frameworks.

This work is partially supported by MURST through project PRIN01-2001021133. We acknowledge preliminary studies on phonons in  $\alpha$ -Ga in collaboration with S. de Gironcoli, G.L. Chiarotti and E. Tosatti.

## References

1. R.W.G. Wyckoff, *Crystal Structures*, 2nd. edn. (Wiley, New York, 1962), Vol. I, p. 22
2. A word of caution is in order: of the six possible ways to assign  $a$ ,  $b$ ,  $c$  to the three crystal axes, at least three different versions can be found in literature. Here, in order to conform to recent experimental works we follow the crystallographic convention ( $Cmca$  symmetry) while in our previous works [10, 22] we followed the historic (pseudotetragonal) convention. In the latter case the  $b$  and  $\bar{c}$  axis are reversed
3. For points and directions of the Brillouin Zone, we have used the standard notation for the  $Cmca$  space group (N. 64) as reported for instance in reference [23], as opposed to the experimental work of reference [12] where the notation for the non-standard  $Bbcm$  setting has been used
4. V. Heine, *J. Phys. C* **1**, 222 (1968)
5. J.E. Inglesfield, *J. Phys. C* **1**, 1337 (1968)
6. R.W. Powell, M.J. Woodman, R.P. Tye, *Br. J. Appl. Phys.* **14**, 432 (1963)
7. O. Hundery, R. Ryberg, *J. Phys. F* **4**, 2084 (1974); R. Kofman, P. Cheyssac, J. Richard, *Phys. Rev. B* **16**, 5216 (1977)
8. F. Greuter, P. Oelhafen, *Z. Physik B* **34**, 123 (1979); S.R. Barman, D.D Sarma, *Phys. Rev. B* **51**, 4007 (1995)
9. W.A. Reed, *Phys. Rev.* **188**, 1184 (1969)

10. M. Bernasconi, G.L. Chiarotti, E. Tosatti, Phys. Rev. B **52**, 9988 (1995)
11. Ch. Sondergaard et al., Phys. Rev. B **67**, 205105 (2003)
12. Landolt-Börnstein, New Series, Group III, Vol. 13, Subvolume a, pp. 57–60, [Reichardt et al., Bull. Am. Phys. Soc. **14**, 378 (1969), and unpublished]
13. S. Baroni, S. de Gironcoli, A. Dal Corso, P. Giannozzi, Rev. Mod. Phys. **73**, 515 (2001)
14. We used the PWSCF and PHONON codes developed by S. Baroni, P. Giannozzi, S. de Gironcoli, A. Dal Corso and others [13]: <http://www.pwscf.org>
15. S. de Gironcoli, Phys. Rev. B **51**, 6773 (1995)
16. K.R. Lyall, J.F. Cochran, Canad. J. Physics **49**, 1075 (1971)
17. D. Vanderbilt, Phys. Rev. B **41**, 7892 (1990)
18. H.J. Monkhorst, J.D. Pack, Phys. Rev. B **13**, 5188 (1976)
19. M. Methfessel, A.T. Paxton, Phys. Rev. B **40**, 3616 (1989)
20. F.D. Murnaghan, Proc. Nat. Acad. Sci. USA **30**, 244 (1944)
21. A.D. Becke, Phys. Rev. A **38**, 3098 (1988); J.P. Perdew, Phys. Rev. B **33**, 8822 (1986)
22. M. Bernasconi, G.L. Chiarotti, E. Tosatti, Phys. Rev. B **52**, 9999 (1995); *ibidem*, Phys. Rev. Lett. **70**, 3295 (1993)
23. J. Zak, *Irreducible Representations of Space Groups* (Benjamin, New York 1969)